

# Optics and non-linear beam dynamics at 4 and 6.5 TeV

R. Tom  s, T. Bach, P. Hagen, A. Langner, Y.I. Levinsen, M.J. McAteer, E.H. Maclean, T.H.B. Persson,  
P. Skowronski and S. White

## Abstract

2012 has been an extraordinary year for the control and understanding of the LHC optics. A record low  $\beta$ -beating of about 7% has been achieved during nominal operation. Consequently the luminosity imbalance between the two main experiments has also achieved a record low value. Magnet experts have found 1% gradient errors in some MQY quadrupoles, which are in good agreement with the beam-based optics corrections. A large effort has been put into probing the polarity of the non-linear correction circuits. So far more than 60 sextupolar and octupolar circuits have been probed revealing some inconsistencies. A large collection of new optics has been tested, including the post LS1 baseline  $\beta^*=0.4$  m. Dedicated MDs have brought first time achievements in the LHC non-linear beam dynamics regime, namely: (i) measurement of DA at injection, (ii) chromatic coupling correction, (iii) IR non-linear corrections at  $\beta^*=0.6$  m, and (iv) the direct measurement of amplitude detuning with AC dipoles. All of these accomplishments give a comfortable basis to make projections and recommendations towards 6.5 TeV.

## 1 RECORD LOW $\beta$ -BEATING

High energy colliders have not traditionally required high precision control of their optics. The maximum relative deviation of the  $\beta$ -function with respect to the model ( $\beta$ -beating) is an appropriate figure of merit to compare different colliders. An illustration of the achieved peak  $\beta$ -beating in various high energy colliders is shown in Table 1 as collected during the “Optics Measurements, Corrections and Modeling for High-Performance Storage Rings” workshop [1]. References for the various machines on the table are: PEP II [2], LEP [3], KEKB [4], CESR [5], HERA-p [6], Tevatron [7] and RHIC [8]. The record low  $\beta$ -beating is held by CESR, the smallest of these colliders with a 768 m circumference. The achieved peak  $\beta$ -beating in these machines is far from the 1-2% in modern light sources such as DIAMOND [9], SOLEIL [10] and ALBA [11].

A 10% peak  $\beta$ -beating at top energy was already demonstrated in the LHC in 2010 [12]. However, owing to the change in the hysteresis branch of some quadrupoles involved in the correction, it was not possible to keep this 10%  $\beta$ -beating during regular operation. In 2011 this technical obstacle was solved [13] and a  $\beta$ -beating near 10% became operational [14, 15]. 2011 started with a  $\beta^*=1.5$  m and intensive optics corrections following the same strategies as in [12]. In August a beta squeeze down to  $\beta^*=1$  m was successfully commissioned [15], apparently without

requiring further optics corrections, although precise  $\beta^*$  measurements were not performed. Between these two periods of different  $\beta^*$  the luminosity imbalance between the ATLAS and CMS experiments increased from roughly 5% to 10% [16] (providing more luminosity for CMS). Squeezing further down to 0.6 m in 2012 could have increased the luminosity imbalance to intolerable levels. It was therefore decided to place special attention to the optics commissioning following the procedure below:

1. Measure the machine in the absence of any beam-based corrections (*virgin* machine) throughout the entire magnetic cycle.
2. Reduce the measurement uncertainty compared to previous years by increasing the excitation amplitude of the AC dipole.
3. Compute new local IR corrections, which can remain constant throughout the beta squeeze process.
4. Compute global corrections to minimize  $\beta$ -beating and dispersion beating simultaneously.
5. Use of local  $\beta^*$  and IP waist knobs to equalize luminosities if required. These knobs must use independently powered quadrupoles excluding the triplet quadrupoles as these act on both beams.

All  $\beta$ -beating and coupling corrections prior to 2012 were removed all along the LHC magnetic cycle. The LHC AC dipoles [17] were used to measure the  $\beta$ -functions along the  $\beta^*$ -squeeze process. A peak  $\beta$ -beating of about 100% is reached for  $\beta^*=0.6$  m. The  $\beta$ -beating rms and peak values corresponding to all measurements during the  $\beta$ -squeeze are shown in Fig. 1. A monotonic increase of the peak and rms values is observed while reducing  $\beta^*$ , suggesting the need for local optics corrections in the Interaction Regions (IRs).

Local corrections are best suited for the IRs where the  $\beta$  functions are large and there are independently powered quadrupoles. However, the small phase advance between quadrupoles introduces some degeneracy in the possible corrections. To minimize the level of degeneracy, multiple optics were corrected simultaneously for both beams in 2012. Figure 2 shows an illustration of a simultaneous correction for six different optics (three per beam) using the segment-by-segment technique [18] for IR5. The good quality of the corrections, as illustrated in Fig. 2, in this tightly constrained scenario provides confidence in this approach.

Global corrections are required to take care of the optics errors in the arcs and the residuals from the IR local corrections. All available singly powered quadrupoles were used

| Lepton Collider | Circumference [km] | Peak $\Delta\beta/\beta$ [%] | Hadron Collider | Circumference [km] | Peak $\Delta\beta/\beta$ [%] |
|-----------------|--------------------|------------------------------|-----------------|--------------------|------------------------------|
| PEP II          | 2.2                | 30                           | HERA-p          | 6.3                | 20                           |
| LEP             | 27                 | 20                           | Tevatron        | 6.3                | 20                           |
| KEKB            | 3                  | 20                           | RHIC            | 3.8                | 20                           |
| CESR            | 0.8                | 7                            | LHC             | 27                 | 7                            |

Table 1: Peak  $\beta$ -beating of various high energy colliders as collected during the Optics Measurements, Corrections and Modeling for High Performance Storage Rings workshop [1].

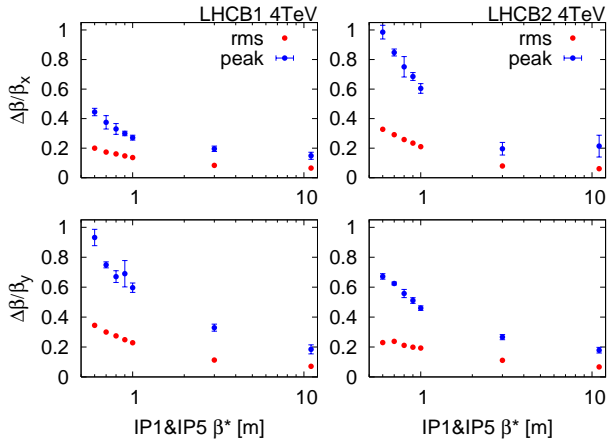


Figure 1:  $\beta$ -beating of the virgin machine along the squeeze. Beam 1 (left) and Beam 2 (right), horizontal (top) and vertical (bottom) plots showing the peak and rms  $\beta$ -beating values versus  $\beta^*$ .

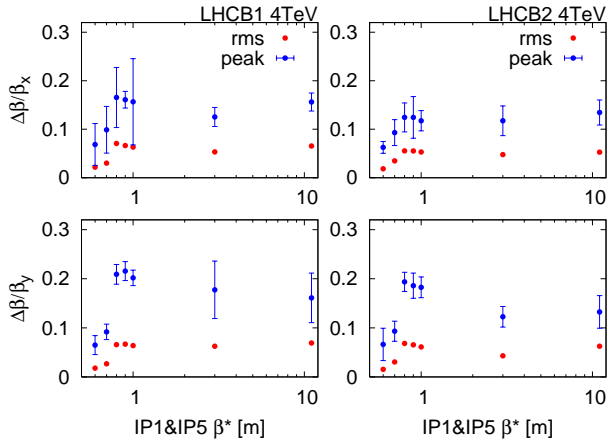


Figure 3:  $\beta$ -beating after local and global corrections along the squeeze. Beam 1 (left) and Beam 2 (right), horizontal (top) and vertical (bottom) plots showing the peak and rms  $\beta$ -beating values versus  $\beta^*$ .

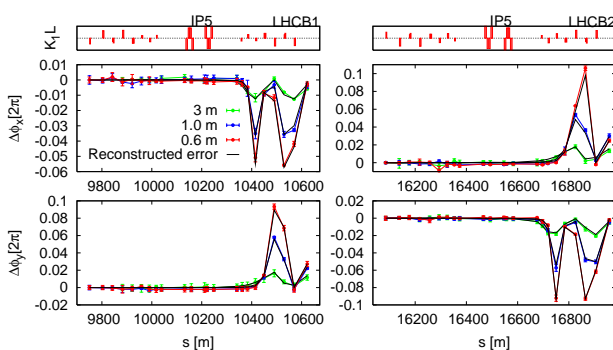


Figure 2: Illustration of the segment-by-segment technique applied to IR5 simultaneously to the two beams and three different  $\beta^*$ . The black lines show the reconstructed error model.

to minimize the  $\beta$ -beating and the normalized dispersion beating at all BPMs in an inverse response matrix approach. Figure 3 shows the evolution of the  $\beta$ -beating along the squeeze after local and global corrections. The record low  $\beta$ -beating of about 7% is reached for  $\beta^* = 0.6$  m; see [18] for further details.

## 2 COUPLING CORRECTION

The global coupling knobs for Beam 2 were improved before the 2012 run by optimizing their performance in computer simulations using their orthogonality and required skew quadrupole strength as figures of merit. The new knobs required substantially less strength of the skew quadrupole while providing a better orthogonality to the complex space of  $f_{1001}$  [19].

From the measurements of the the virgin machine new local coupling corrections were calculated for 2012. The local corrections have remained very constant throughout the magnetic cycle and very stable throughout the year. This is of big importance, for the use of the global knobs requires that the strong local sources are corrected.

The global knobs are used by the shift crew in an iterative manner to correct the coupling. The best setting is found by testing different settings of the global knobs while observing the  $|C^-|$  in the TuneViewer [20]. This can be time consuming operation. The fact that the measurement is based on a pickup at a single location is also a limiting factor. This is because minimizing the coupling at this location might not be the same as minimize the coupling globally.

In 2012 a new software to measure the coupling from the

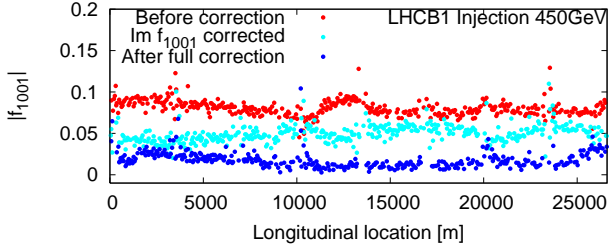


Figure 4: Coupling corrections using the turn-by-turn from the pilot injections in the LHC.

injections oscillations was developed. It uses the recorded turn-by-turn data for the first 1000 turns after an injection to calculate the  $f_{1001}$  at each individual BPM. It uses the undamped oscillations from the pilot bunches that are preceding every fill in the LHC. From the  $f_{1001}$  the optimum setting for the coupling knobs are calculated and presented in the software. This correction scheme has now been tested for both beams and proven itself successful in normal operation of the LHC. An example of a correction using this method is shown in Figure 4. In this case the correction was done in two steps, first correcting the imaginary part of the  $f_{1001}$ , and then later correcting the real as well as the imaginary part. However, in normal operation both parts of the  $f_{1001}$  can be corrected simultaneously. The corrections were successful and the results were in good agreement with the values received from the TuneViewer system. Hence, we can conclude that we were able to reduce the  $|C^-|$  by about a factor 4. In 2011 there was a problem with large drifts of the coupling of Beam 2. In 2012 this problem seems to have disappeared and the need to change the coupling knobs is now less frequent.

### 3 MQY 1% CALIBRATION ERRORS

After revising the FiDeL existing magnetic measurements and the LHC LSA databases, inconsistencies of up to 1.5% were found in the transfer function of some MQY magnets. These errors seem in good agreement with those previously found from the optics measurement [18]. Table 2 compares the errors found from magnetic measurements (FiDeL) to the values from beam-based optics corrections. In most cases similar errors are found by both methods. The largest discrepancy (marked in red in the table) is for a rather strong error in IR8. The beam-based correction used a quadrupole right of IP8 while FiDeL finds an error in a quadrupole left of IP8.

In order to experimentally verify that the new FiDeL predictions are correct an MD was performed in November 2012. The magnet strength of the MQY quadrupoles was corrected according to the suggestions from FiDeL. The correction was performed via a knob in a virgin machine, without any other corrections, and starting from the pre-cycle up to the energy of 4 TeV to avoid any hysteresis effects. No beta-squeeze was performed during this MD.

| Quad beam2 | b-based [ $10^{-4}$ ] | FiDeL [ $10^{-4}$ ] | Quad beam1 | b-based [ $10^{-4}$ ] | FiDeL [ $10^{-4}$ ] |
|------------|-----------------------|---------------------|------------|-----------------------|---------------------|
| q4.11      | 13                    | 0                   | q4.11      | 0                     | 0                   |
| q4.r1      | 0                     | 0                   | q4.r1      | 0                     | 0                   |
| q4.12      | 0                     | 0                   | q4.r2      | 0                     | 0                   |
| q4.r2      | 0                     | 0                   | q4.12      | 0                     | 0                   |
| q5.12      | 0                     | 36                  | q5.12      | 0                     | 41                  |
| q5.14      | 0                     | 0                   | q5.14      | 0                     | 0                   |
| q6.r4      | 0                     | 0                   | q6.r4      | 0                     | 0                   |
| q6.14      | 0                     | 61                  | q5.r4      | 0                     | 21                  |
| q5.r4      | 0                     | 10                  | q6.14      | 0                     | 72                  |
| q4.15      | 100                   | 153                 | q4.15      | 0                     | 32                  |
| q4.r5      | 0                     | 0                   | q4.r5      | 0                     | 0                   |
| q5.r6      | 10                    | 0                   | q5.16      | 60                    | 72                  |
| q4.16      | 0                     | 0                   | q4.r6      | 0                     | 0                   |
| q5.16      | 70                    | 73                  | q5.r6      | 10                    | 0                   |
| q4.r6      | 0                     | 0                   | q4.16      | 0                     | 0                   |
| q5.r8      | 80                    | 95                  | q4.r8      | 0                     | 0                   |
| q4.18      | 0                     | 119                 | q4.18      | 100                   | 122                 |
| q4.r8      | 240                   | 0                   | q5.r8      | 270                   | 99                  |

Table 2: MQY errors as seen from beam-based optics corrections (b-based column) and FiDeL magnetic measurements. The largest discrepancy between these two approaches is marked in red.

Optics measurements with the AC dipole were carried out at flat-top. Figure 5 compares the resulting local phase-beating to measurements before the optics commissioning in 2012 for IR6 and IR8 of Beam 1. A clear improvement is achieved with the new calibrations. These improvements are also seen for other IRs and represent the experimental verification of the new MQY calibration.

### 4 POLARITY CHECKS

Polarities and strengths of the focusing and defocusing octupoles (MOF and MOD), spool piece octupole correctors (MCO), arc skew sextupole correctors (MSS), and interaction region sextupoles (MCSX and MCSSX) have been extensively checked. Table 3 summarizes the results of all the polarity checks.

Each arc contains between 8 and 13 octupoles of each of types MOF and MOD, and 77 type MCO. All octupoles of a type in each arc are powered as a group. More details about these magnets can be found in [21]. The polarity of each octupole group in each arc was verified by trimming one group and measuring the resulting change in second order chromaticity. In each case the measured second order chromaticity agreed well with predicted value, indicating that all octupoles have the correct polarity.

Each arc contains four skew sextupoles MSS, powered as a group. The MSS polarities were checked by measuring the change to chromatic coupling when a magnet family was trimmed. A comparison of the measured chro-

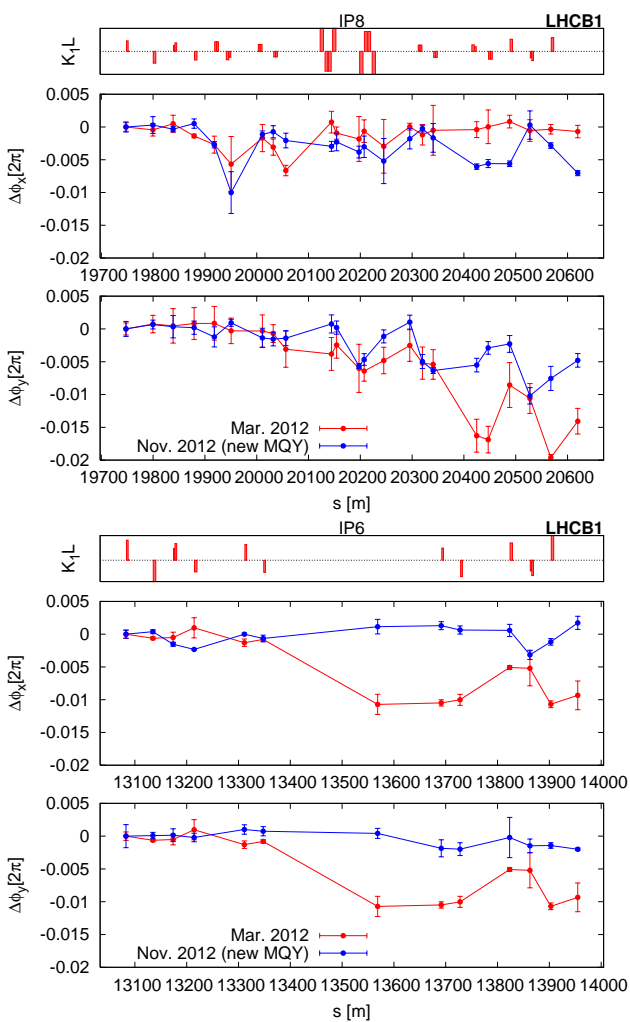


Figure 5: Phase beating with the old (red) and the new MQY calibrations (blue) for IR8 (top) and IR6 (bottom), showing a clear improvement with the new calibrations.

matic coupling with model predictions indicated that all measured MSS magnets have reversed polarity.

Each interaction region contains pairs of normal sextupole correctors MCSX and skew sextupole correctors MCSSX. The polarities of the skew sextupoles in IR1, where the crossing angle is vertical, and the normal sextupoles in IR5, where the crossing angle is horizontal, were verified by trimming the magnets and measuring the resulting tune shifts. Comparison of the measured tune shifts with model predictions shows that the polarities of MCSSX in IR1 and MCSX in IR5 are correct.

## 5 DA MEASUREMENT AT INJECTION

During the June 2012 MD block non-linear optics studies were performed on LHC Beam 2 at injection. The Aperture Kicker (MKQA) was used to excite high amplitude betatron oscillations for the measurement of the dynamic aperture (DA) and first and second order anharmonicities.

| Type  | Location | polarity | Location | polarity |
|-------|----------|----------|----------|----------|
| MOF   | A12 B1   | Correct  | A12 B2   | Correct  |
| MOF   | A23 B1   | Correct  | A23 B2   | Correct  |
| MOF   | A34 B1   | Correct  | A34 B2   | Correct  |
| MOF   | A45 B1   | Correct  | A45 B2   | Correct  |
| MOF   | A56 B1   | Correct  | A56 B2   | Correct  |
| MOF   | A67 B1   | Correct  | A67 B2   | Correct  |
| MOF   | A78 B1   | Correct  | A78 B2   | Correct  |
| MOF   | A81 B1   | Correct  | A81 B2   | Correct  |
| MOD   | A12 B1   | Correct  | A12 B2   | Correct  |
| MOD   | A23 B1   | Correct  | A23 B2   | Correct  |
| MOD   | A34 B1   | Correct  | A34 B2   | Correct  |
| MOD   | A45 B1   | Correct  | A45 B2   | Correct  |
| MOD   | A56 B1   | Correct  | A56 B2   | Correct  |
| MOD   | A67 B1   | Correct  | A67 B2   | Correct  |
| MOD   | A78 B1   | Correct  | A78 B2   | Correct  |
| MOD   | A81 B1   | Correct  | A81 B2   | Correct  |
| MCO   | A12 B1   | NA       | A12 B2   | NA       |
| MCO   | A23 B1   | Correct  | A23 B2   | Correct  |
| MCO   | A34 B1   | Correct  | A34 B2   | Correct  |
| MCO   | A45 B1   | Correct  | A45 B2   | Correct  |
| MCO   | A56 B1   | Correct  | A56 B2   | Correct  |
| MCO   | A67 B1   | Correct  | A67 B2   | Correct  |
| MCO   | A78 B1   | Correct  | A78 B2   | NA       |
| MCO   | A81 B1   | Correct  | A81 B2   | NA       |
| MSS   | A12 B1   | Reversed | A12 B2   | Reversed |
| MSS   | A23 B1   | Reversed | A23 B2   | Reversed |
| MSS   | A34 B1   | Reversed | A34 B2   | Reversed |
| MSS   | A45 B1   | -        | A45 B2   | Reversed |
| MSS   | A56 B1   | -        | A56 B2   | Reversed |
| MSS   | A67 B1   | -        | A67 B2   | Reversed |
| MSS   | A78 B1   | -        | A78 B2   | -        |
| MSS   | A81 B1   | NA       | A81 B2   | -        |
| MCSSX | L1       | Correct  | R1       | Correct  |
| MCSX  | L5       | Correct  | R5       | Correct  |
| MQS   | A23 B1   | Reversed | R2 B2    | Reversed |
| MQS   | A45 B1   | Reversed | R4 B2    | Reversed |
| MQS   | A67 B1   | Reversed | R6 B2    | Reversed |
| MQS   | A81 B1   | Reversed | R8 B2    | Reversed |
| MQS   | L2 B1    | Reversed | L1 B2    | Reversed |
| MQS   | L6 B1    | Reversed | L3 B2    | Reversed |
| MQS   | L8 B1    | Reversed | L5 B2    | Reversed |
| MQS   | R1 B1    | Reversed | L7 B2    | Reversed |
| MQS   | R5 B1    | Reversed | A12 B2   | Reversed |
| MQS   | R7 B1    | Reversed | A78 B2   | Reversed |
| MQS   | A56 B2   | Reversed | -        | -        |
| MQSX  | L1       | Reversed | R1       | Reversed |
| MQSX  | L2       | Reversed | R2       | Reversed |
| MQSX  | L5       | Reversed | R5       | Reversed |
| MQSX  | L8       | Reversed | R8       | Reversed |

Table 3: Polarities of arc octupoles, arc sextupoles, and interaction region sextupoles as resulting from beam-based comparisons between LSA and MAD. “NA” stands for not available and the sign “-” means that the corresponding circuit was not tested.

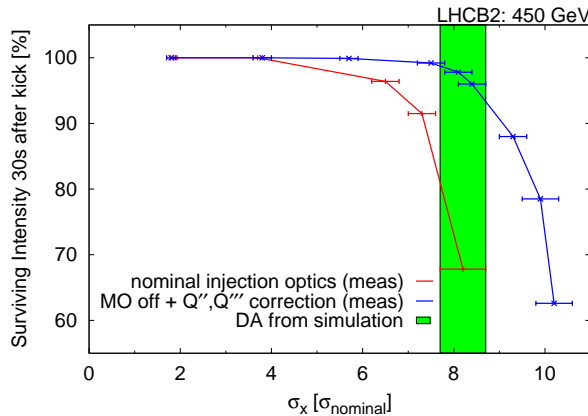


Figure 6: Surviving beam intensity 30 seconds after a transverse kick versus the amplitude of the kick for the nominal (red) and the corrected (blue) machines. The simulated dynamic aperture is also shown corresponding to the nominal machine during the first part of the year with the defocusing polarity in the MO Landau octupoles.

Measurements were performed on the nominal injection settings, and with the Landau octupoles (MO) depowered and  $Q''$  and  $Q'''$  corrections applied to obtain as linear a machine as possible.

By examining how losses experienced by the beam varied with amplitude of excitation it is possible to determine the DA. In particular by linearising the machine in the second stage of the MD and repeating the measurement, the effect of the DA was clearly revealed. Figure 6 shows the surviving beam intensity following horizontal excitation with the MKQA versus the amplitude of excitation. Our best available model of the LHC (which well reproduces the measured detuning with amplitude) has been used to perform DA simulations with SIXTRACK. The result of this simulation was found to be  $8.2 \pm 0.5\sigma_{\text{nominal}}$ <sup>1</sup> and is also displayed in Figure 6. Our measurements and simulation are in excellent agreement.

Later in 2012 the polarity of the MO were reversed for operation. Figure 7 shows the results of SIXTRACK simulations with our best model for both polarities of MO, showing a clear improvement with the new polarity.

## 6 CHROMATIC COUPLING CORRECTION

The systematic skew sextupole components in the dipoles are known to cause significant chromatic coupling if left uncorrected. There are several skew sextupoles installed to compensate for this known systematic effect [22]. The spurious skew sextupole errors will produce additional chromatic coupling since the dispersion is largely horizontal. Normal sextupoles produce chromatic coupling in regions of vertical dispersion. Once linear coupling is well

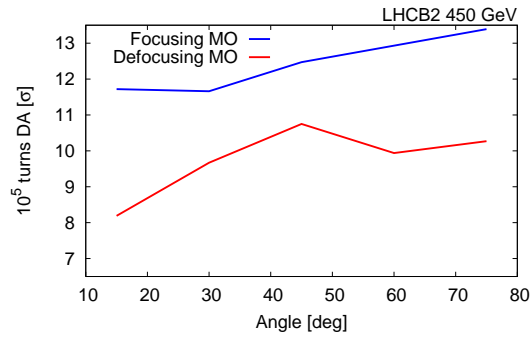


Figure 7: Dynamic aperture at injection with nominal tunes and for the two polarities of the Landau octupoles. The defocusing MO corresponds to the MO polarity during the first part of the year.

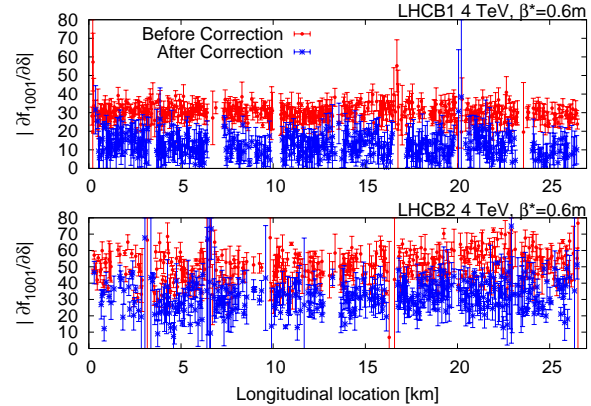


Figure 8: First chromatic coupling correction in the LHC for Beam 1 (top) and Beam 2 (bottom).

corrected, chromatic coupling should be corrected as well for optimal machine performance.

In 2012 the first beam based chromatic coupling correction was performed in the LHC. The correction was tested for the nominal 2012 optics, meaning a  $\beta^* = 0.6\text{ m}$ . Beam 2 had 9 independent skew sextupole circuits while Beam 1 had 8 available at this time. In Figure 8 the chromatic coupling before and after correction are presented. The weighted mean value of  $\partial f_{1001}/\partial \delta$  was measured to be somewhat larger for Beam 2 than Beam 1, approximately 50 units for beam 2 and 30 units for Beam 1. The chromatic  $f_{1001}$  was decreased by about 20 units for both beams, proving that the corrections were successful.

## 7 IR NON-LINEAR CORRECTION

Non-linear errors in the the LHC IRs may have a significant detrimental impact on lifetime and dynamic aperture. By examining the feed down to tunes and free coupling while varying the crossing angles in IP1 and IP5, we have performed first attempts at the local correction of higher order magnetic errors in the LHC IRs.

Table 4 displays the feed down to tune and coupling from higher order multipoles for horizontal and vertical

<sup>1</sup>By  $\sigma_{\text{nominal}}$  we refer to the beam size with normalized emittance of  $\epsilon = 3.75 \mu\text{m}$ .

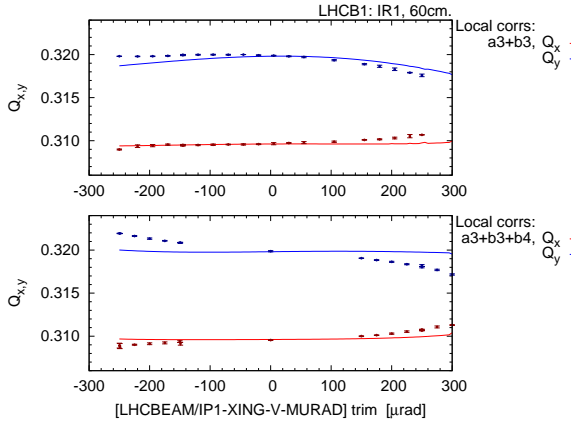


Figure 9: Beam 1 tunes vs IP1 crossing angle from measurement and simulation with  $a_3 + b_3$  and  $a_3 + b_3 + b_4$  correction applied.

excursions.

Table 4: Tune ( $\Delta Q$ ) and Coupling ( $\Delta C$ ) feed down from non-linear Multipoles

|               | $b_3$      | $a_3$      | $b_4$      | $a_4$      | $b_5$      | $a_5$      | $b_6$      |
|---------------|------------|------------|------------|------------|------------|------------|------------|
| <b>H bump</b> | $\Delta Q$ | $\Delta C$ | $\Delta Q$ | $\Delta C$ | $\Delta Q$ | $\Delta C$ | $\Delta Q$ |
| <b>V bump</b> | $\Delta C$ | $\Delta Q$ | $\Delta Q$ | $\Delta C$ | $\Delta C$ | $\Delta Q$ | $\Delta Q$ |

Measurements performed on the uncorrected machine during the  $\beta^* = 0.6$  m MD in November 2012 showed a good agreement with simulations incorporating magnetic measurements of the errors in the IRs. The magnetic measurements were therefore used for the calculation of local corrections of the  $b_3$ ,  $a_3$  and  $b_4$  multipoles in IP1 and IP5.

During dedicated MD time the crossing angles in IP1 and 5 (vertical and horizontal respectively) were varied, firstly with  $a_3 + b_3$  corrections applied, then on further addition of the  $b_4$  correction. The tunes as measured by the LHC BBQ system and found in simulation, are plotted versus the IP1 crossing angle in Figures 9 and 10 for Beam 1 and 2 respectively.

The coupling data was of too low quality to draw any conclusions; however the method has previously been successful observing feed down from errors in IP2. Analysis of IP5 data is ongoing.

Measurement and simulation with  $a_3 + b_3$  corrections applied show a good agreement for both beams (note however that this verifies only the  $a_3$  correction in IP1: the  $b_3$  feeds down to coupling for a vertical excursion). On applying the  $b_4$  correction, measurement and simulation remain in good agreement for Beam 2; however Beam 1 displays a large linear discrepancy in the variation of tune with crossing angle. This may be explained by a  $\sim 5$ mm vertical misalignment of the  $b_4$  corrector with respect to the  $b_4$  sources. Results of simulation incorporating such a mis-

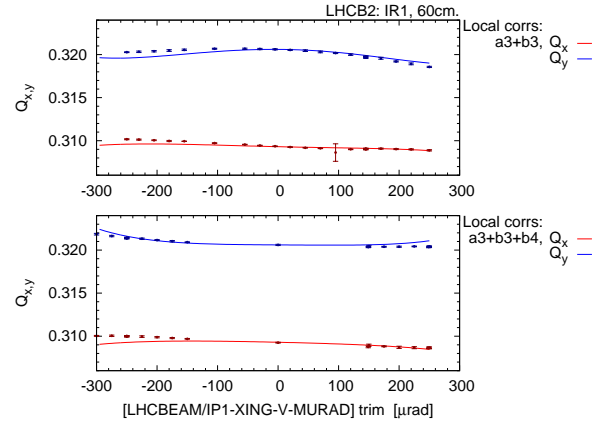


Figure 10: Beam 2 tunes vs IP1 crossing angle from measurement and simulation with  $a_3 + b_3$  and  $a_3 + b_3 + b_4$  correction applied.

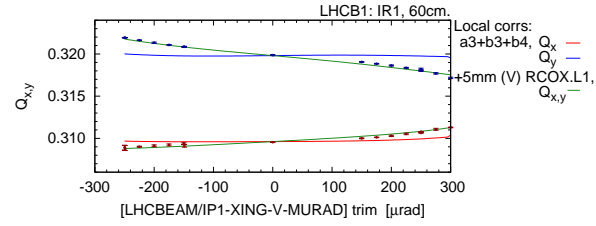


Figure 11: Beam 1 tunes vs IP1 crossing angle from measurement and simulation with  $a_3 + b_3 + b_4$  corrections applied and a 5mm vertical misalignment of the  $b_4$  corrector.

alignment are shown in Figure 11, which is seen to be in good agreement with the measurements.

The additional  $a_3$  component resulting from feed-down from the  $b_4$  corrector must be incorporated in any final correction scheme, however these results demonstrate the feasibility of applying this method to the LHC.

## 8 MEASUREMENT OF AMPLITUDE DETUNING

The amplitude detuning is a critical parameter for the understanding and control of beam instabilities. Yet, measuring the amplitude detuning at top energy represents a real challenge as the only available excitors that can provide a few sigmas oscillation are the AC dipoles. Furthermore, the AC dipoles force oscillations at frequencies different from the natural tunes of the machine and, ideally, the machine tunes should not be excited during the flat-top. We relied on the residual non-adiabaticity of the AC dipole ramping process to measure the tunes during a dedicated MD in 2012. The actual observation of the machine tunes required aggressive cleaning using SVD techniques. The measured horizontal and vertical tunes are shown in Fig. 12 versus the horizontal oscillation amplitude for Beam 2. This represents the first successful direct measurement of amplitude detuning with AC dipoles. The comparison to model pre-

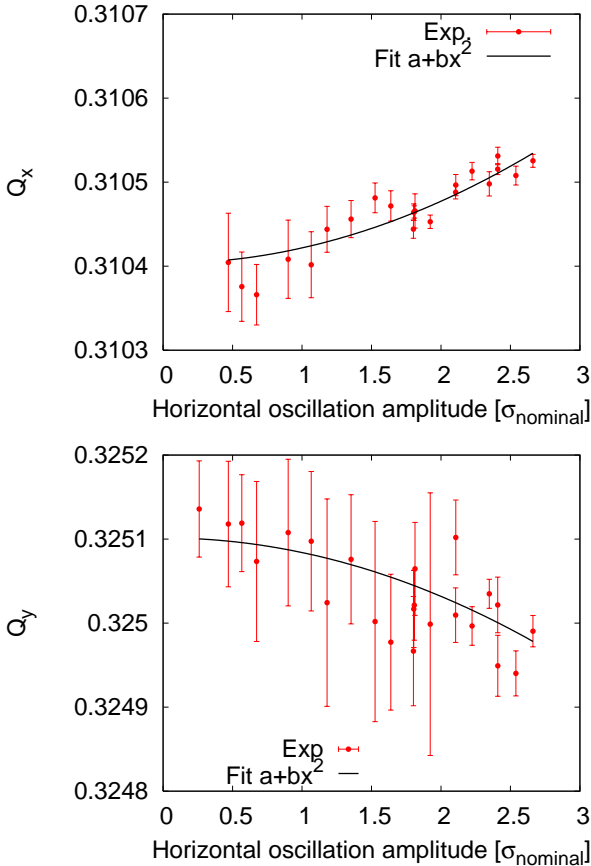


Figure 12: Beam 2 horizontal (top) and vertical (bottom) amplitude detuning versus the horizontal oscillation amplitude as measured during 2012 MDs at  $\beta^*=0.6$  m together with quadratic fits.

diction is under study [23].

## 9 OPTICS MEASUREMENTS AT $\beta^*=0.4$ M

During the 2012 MDs two different optics featuring  $\beta^*=0.4$  m were tested and measured in the LHC. One optics corresponds to the continuation of the nominal squeeze and the other uses the ATS [24]. In both cases IR local corrections were implemented while global corrections were considered less critical and, consequently, they were not applied. The  $\beta$ -beating from these optics is compared in Fig. 13, both showing similarly acceptable levels of  $\beta$ -beating.

The off-momentum optics aberrations have been a concern for the LHC machine protection at low  $\beta^*$  values since these could degrade the collimation performance. A direct measurement of the off-momentum  $\beta$ -beating for the nominal optics at  $\beta^*=0.4$  m is shown in Fig. 14. Measurement and model predictions are in very good agreement.

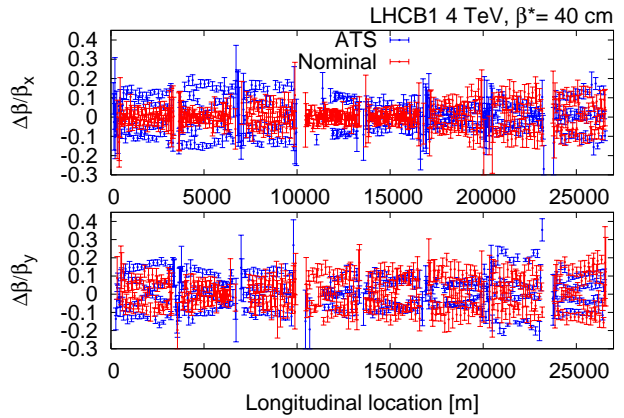


Figure 13: Horizontal (top) and vertical (bottom)  $\beta$ -beating as measured during 2012 MDs for two different optics at  $\beta^*=0.4$  m.

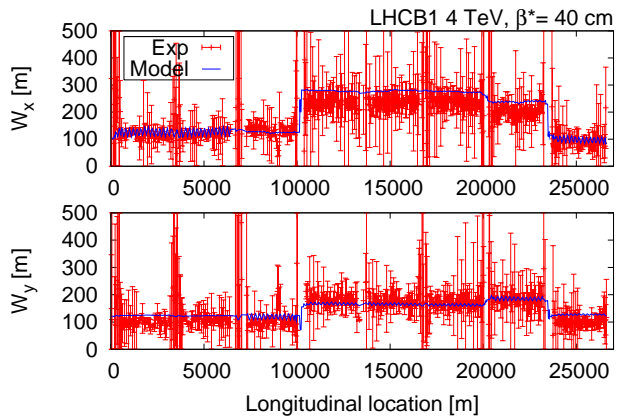


Figure 14: Chromatic  $\beta$ -beating (Montague function) for the nominal LHC optics at  $\beta^*=0.4$  m compared to the model prediction (blue line).

## 10 INJECTION TUNES AND $\beta^*$ AFTER LS1

The first step of the LHC beta-squeeze at top energy consists in shifting the fractional tunes between the injection (0.28, 0.31) and collision (0.31, 0.32) working points. Figure 15 shows the tune jump crossing 7<sup>th</sup> and 10<sup>th</sup> order resonances. This was decided to reduce the effects from transverse coupling at injection and during the energy ramp, and to profit from the larger Dynamic Aperture at the injection tunes [25, 26]. However, nowadays this tune jump is found to be too violent for the orbit feedback and, furthermore, in the scenario of a smaller  $\beta^*$  at injection and/or at flat-top the tune jump would be seen as even more violent (not only for the orbit feedback but also for beam losses due to stronger resonances). A possible way to avoid losing the orbit feedback during the tune jump would be to lengthen the time used for the jump. This would cause softer changes in the orbit but, on the other hand, it would increase the time that the beams sit on the 7<sup>th</sup> and 10<sup>th</sup> order

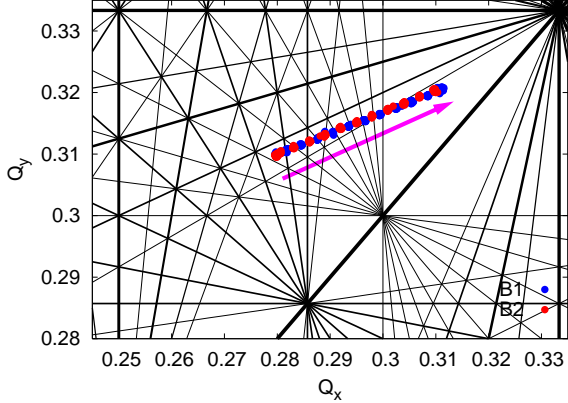


Figure 15: Tune jump between injection and collision tunes together with the relevant resonances.

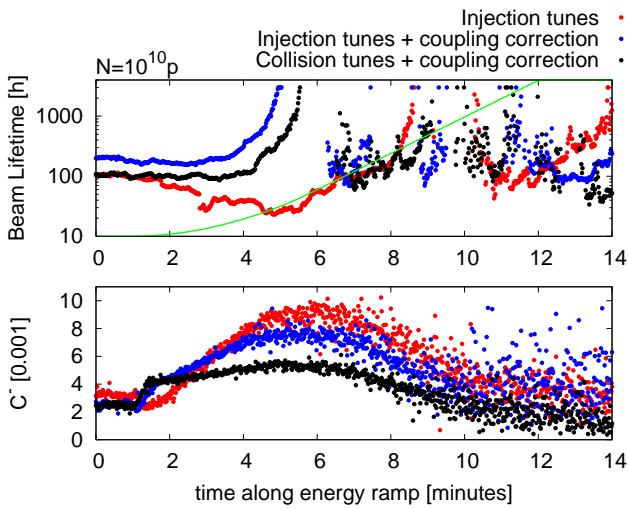


Figure 16: Comparison of lifetime and coupling along 3 energy ramps with injection tunes (2 successive coupling corrections) and collision tunes.

resonances.

The feasibility of injecting and ramping with collision tunes was already demonstrated during the MDs of 2011 [27]. Figure 16 shows how after correcting the transverse coupling along the energy ramp the collision tunes performed as well as the injection tunes in terms of lifetime.

As shown in Section 5 Landau octupoles have an impact on dynamic aperture. Figure 17 shows the DA using collision tunes at injection for the two 2012 octupole settings. This is to be compared to Fig. 7 with nominal injection tunes. For the defocusing octupole polarity (used during the first months of 2012) a DA increase of about  $4\sigma$  is observed moving to the collision tunes. For the focusing octupole polarity (used towards the end of 2012) a reduction of about  $1\sigma$  is observed. In the scenario of using collision tunes and the octupole focusing polarity a reduction of the octupole strength should be investigated in order not to lose

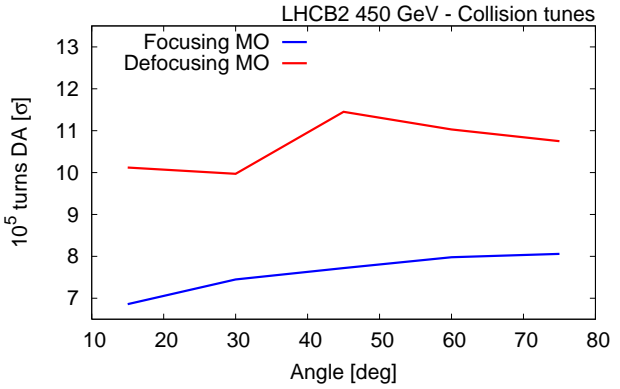


Figure 17: Dynamic aperture at injection with collision tunes and for the two polarities of the Landau octupoles.

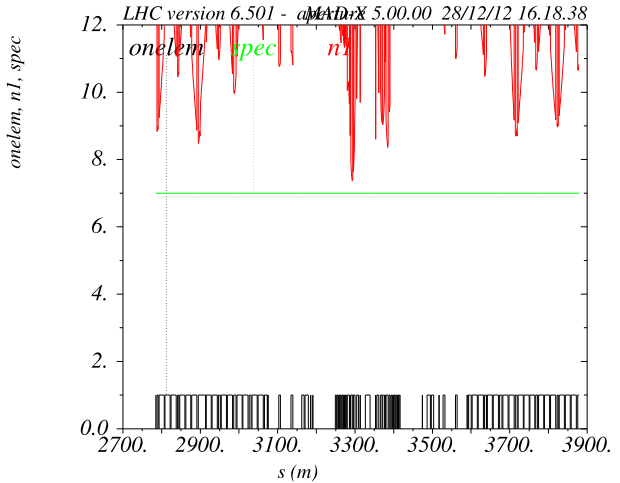


Figure 18: Aperture in terms of  $N_1$  for Beam 1 and IR5. The used parameters are:  $\epsilon_{x,y} = 3\mu\text{m}$ , c.o. = 3mm,  $\frac{dp}{p} = 0.5\%$ ,  $\theta = 190\mu\text{m}$ .

this  $1\sigma$  in the DA. As a matter of fact the strength of the octupoles at injection was not optimized during 2012.

In [28] it was already proposed to use collision tunes at injection and reduce a couple of meters the  $\beta^*$  in IP1 and IP5. The minimum  $\beta^*$  at injection is limited by the available aperture in the IR and by the minimum current allowed in the MQY magnets, which is nominally 120 A. This limit is just above the 116 A needed for the  $\beta^* = 5$  m; however, magnet experts would consider acceptable to reduce the 120 A nominal limit to 116 A. The available aperture puts tighter constraints in the  $\beta^*$ . The half crossing angle scales as  $\theta[\mu\text{m}] = 170\sqrt{11\epsilon/(\beta^*3.75)}$ , where  $\epsilon$  is the emittance in  $\mu\text{m}$ . The largest emittance expected in 2015 at injection is  $\epsilon = 3\mu\text{m}$ . This sets a  $\beta^* = 7$  m as an absolute minimum as shown in Fig. 18. However, it might not be needed to push so much the  $\beta^*$  since there will be the possibility to squeeze the  $\beta^*$  during the energy ramp.

## 11 RAMP & SQUEEZE AND COLLIDE & SQUEEZE

The IR2 and IR8 triplets in their injection optics configuration can only be ramped up to 6.45 TeV. Therefore to reach the planned 6.5 TeV after LS1, the optics has to be modified during the energy ramp. This qualitative step in optics control and commissioning should be used to start the beta-squeeze during the ramp and save time for luminosity production. This is known as Ramp & Squeeze [29].

It has been proposed to put the beams in collision before the end of the beta-squeeze. This could help to suppress instabilities and/or to increase integrated luminosity via  $\beta^*$  leveling.

The challenge being faced by both Ramp & Squeeze and Collide & Squeeze is the optics measurement resolution with just a single AC dipole shot (since it has to be run while magnets ramp). Some test measurements during the energy ramp in 2012 revealed about a 10% resolution on the  $\beta$ -functions. Doubling the length of the AC dipole flat-top excitation from 200 ms to 400 ms might be the only way to improve the measurement resolution. Currently it would not be straight forward to reconstruct the optics status of the machine at any given time, e.g. between two matching points during the squeeze. Some tools will need to be developed to address this point.

## 12 DA AND OCTUPOLE REACH AT $\beta^*=0.4$ M

Since MO octupoles were used close to their maximum strength at 4 TeV it is feared that they will not be strong enough for 6.5 or 7 TeV. However it is possible to resort to the inner triplet octupoles to provide extra amplitude detuning. This has the inconvenience that the the inner triplet octupoles affect both beams with opposite effects in the amplitude detuning. Therefore when using these octupoles the maximum amplitude detuning will need to have opposite signs for the two beams. Table 5 shows the maximum amplitude detunings in terms of MO equivalent current for both beams in the two possible configurations. The direct term of the amplitude detuning can be doubled with respect to using only the arc MO octupoles.

In these extreme octupolar configurations a reduction of the single particle dynamic aperture is expected. Figure 19 shows DA calculations in four configurations at 7 TeV and at  $\beta^*=0.4$  m corresponding to: IR correction, No IR correction, Maximum octupole focusing and Maximum octupole defocusing. The ideal configuration is with IR correction, feature the largest DA. Removing the IR non-linear correction reduces the DA by almost  $3\sigma$ . This is a strong reason to make available all inner triplet correctors after LS1. Using all octupoles with the above extreme configurations cause a significant loss of DA even below the settings of the primary collimators. The minimum DA is summarized in Table 6.

|   | Beam 1 | Beam 2 |
|---|--------|--------|
| Maximum focusing in MO, MCO & MCOX                |        |        |
| $\partial Q_x / \partial 2J_x$ [Amps (MO equiv.)] | 1191   | -1012  |
| $\partial Q_y / \partial 2J_y$ [Amps (MO equiv.)] | 619    | -1319  |
| $\partial Q_z / \partial 2J_y$ [Amps (MO equiv.)] | 650    | -2638  |
| Maximum defocusing in MO, MCO & MCOX              |        |        |
| $\partial Q_x / \partial 2J_x$ [Amps (MO equiv.)] | -586   | 1540   |
| $\partial Q_y / \partial 2J_y$ [Amps (MO equiv.)] | -1086  | 1082   |
| $\partial Q_z / \partial 2J_y$ [Amps (MO equiv.)] | -1482  | 1976   |

Table 5: Amplitude detunings for two configurations of the available octupoles in the LHC at 7 TeV yielding a maximum focusing for Beam 1 and a maximum defocusing for Beam 1 at  $\beta^*=0.4$  m.

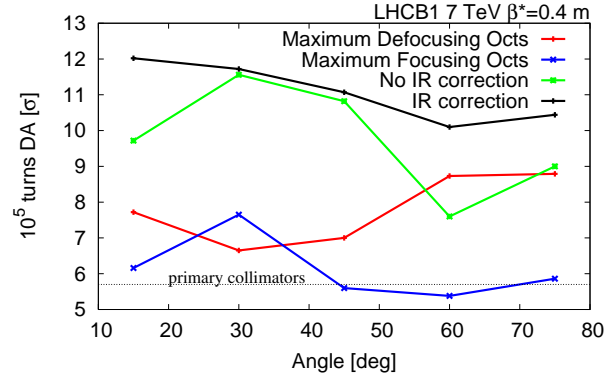


Figure 19: Dynamic aperture at 7 TeV and  $\beta^*=0.4$  m for the bare machine (No IR correction), including IR correction and using the octupolar IR correctors to generate maximum focusing or maximum defocusing amplitude detuning.

## 13 LUMINOSITY PROJECTIONS AT 6.5 TEV

Table 7 shows peak luminosities for various  $\beta^*$  and crossing angles at 6.5 TeV with the 50 ns bunch spacing configuration and assuming normalized emittances of  $\epsilon = 1.6 \mu\text{m}$ . The crossing angle is chosen to provide a separation of  $9.3 \sigma$  in the horizontal plane. The upper part of the table shows luminosities for round beams yielding up to  $2.4 \cdot 10^{34} \text{ cm}^{-2} \text{ s}^{-1}$  with the lowest foreseen  $\beta^*$  of 0.3 m. The lower part of the table shows flat optics with tentative  $\beta^*$ 's that might be achievable if the lowest  $\beta^*$  is set in the plane where the beam chamber has the largest aperture in the triplets. A 23% increase in luminosity might be achievable with flat optics if the corresponding minimum  $\beta^*$  were

|                             | Minimum DA [ $\sigma$ ] |
|-----------------------------|-------------------------|
| IR correction               | 10                      |
| No IR correction            | 7.5                     |
| Maximum octupole focusing   | 5.5                     |
| Maximum octupole defocusing | 6.5                     |

Table 6: Minimum DA for two configurations of the available octupoles for Beam 1 at 7 TeV and  $\beta^*=0.4$  m.

| $\beta_x^*$<br>[m] | $\beta_y^*$<br>[m] | $\theta$<br>[μrad] | Pile-up | Luminosity<br>$[10^{34}\text{cm}^{-2}\text{s}^{-1}]$ | $\Delta$<br>[%] |
|--------------------|--------------------|--------------------|---------|--|-----------------|
| 0.5                | 0.5                | 201                | 110     | 1.90   |                 |
| 0.4                | 0.4                | 225                | 130     | 2.14   | 13              |
| 0.3                | 0.3                | 260                | 150     | 2.41   | 13              |
| 0.6                | 0.4                | 184                | 130     | 2.08   |                 |
| 0.6                | 0.3                | 184                | 140     | 2.40   | 15              |
| 0.6                | 0.2                | 184                | 180     | 2.94   | 23              |

Table 7: Luminosity projections for various  $\beta^*$  and crossing angles at 6.5 TeV with the 50 ns configuration and assuming normalized emittances of  $\epsilon = 1.6 \mu\text{m}$ . The last column shows the relative differential luminosity with respect to the previous row.

| $\beta_x^*$<br>[m] | $\beta_y^*$<br>[m] | $\theta$<br>[μrad] | Pile-up | Luminosity<br>$[10^{34}\text{cm}^{-2}\text{s}^{-1}]$ | $\Delta$<br>[%] |
|--------------------|--------------------|--------------------|---------|--|-----------------|
| 0.5                | 0.5                | 282                | 47      | 1.60   |                 |
| 0.45               | 0.43               | 298                | 50      | 1.71   | 7               |
| 0.37               | 0.33               | 326                | 56      | 1.92   | 12              |
| 0.5                | 0.33               | 282                | 58      | 1.97   |                 |
| 0.5                | 0.23               | 282                | 69      | 2.36   | 20              |

Table 8: Luminosity projections for various  $\beta^*$  and crossing angles at 6.5 TeV with the 25 ns configuration and assuming normalized emittances of  $\epsilon = 1.9 \mu\text{m}$ . The last column shows the relative differential luminosity with respect to the previous row.

avhievable.

Table 8 shows peak luminosities for various  $\beta^*$  and crossing angles at 6.5 TeV with the 25 ns bunch spacing configuration and assuming normalized emittances of  $\epsilon = 1.9 \mu\text{m}$ . The crossing angle is chosen to provide a separation of  $12 \sigma$  in the horizontal plane. The upper part of the table shows luminosities for almost round beams yielding up to  $1.9 \cdot 10^{34}\text{cm}^{-2}\text{s}^{-1}$  with the lowest foreseen  $\beta^*$  of 0.33 m. The lower part of the table shows flat optics with tentative  $\beta^*$ 's that might be achievable if the lowest  $\beta^*$  is set in the plane where the beam chamber has the largest aperture in the triplets. A 20% increase in luminosity might be avhievable with flat optics if the corresponding minimum  $\beta^*$  were avhievable. The 25 ns configuration gives about 20% lower luminosity than the 50% for similar  $\beta^*$  settings. It is important to note that the peak luminosity is almost insensitive to the  $\beta^*$  in the crossing plane between  $\beta^* = 0.37 \text{ m}$  and  $\beta^* = 0.6 \text{ m}$  since a reduction of  $\beta^*$  implies an increase in the crossing angle.

## 14 SUMMARY & OUTLOOK

2012 has been an extraordinary year for the LHC Optics Measurement and Corrections. A long list of first time achievements has been accomplished:

1. Record low beta-beating of 7% for hadron colliders
2. First LHC Dynamic Aperture measurement at injection benchmarking simulations
3. First LHC beam-based chromatic coupling correction improving existing model-based corrections
4. First demonstration of triplet non-linear corrections in LHC
5. First direct measurement of amplitude detuning using AC dipoles.

Furthermore, probably all the quadrupole errors in the 1% level have been identified and the databases will be fixed for 2015. All these accomplishments give a comfortable basis to make projections and recommendations for the post LS1 era. Starting from injection the tunes should be already set to the collision tunes to avoid tune jumps at low  $\beta^*$  since it is foreseen to squeeze during the energy ramp. If the squeeze during the energy ramp needed to be boosted the IP1 and IP5  $\beta^*$  at injection could be reduced to some value above 7 m. The Landau octupoles have a significant impact on the dynamic aperture at injection. The lowest strength needed to suppress instabilities from collective effects should be used. The optics measurements during the ramp and squeeze with the 2012 performance would not be good enough to guarantee corrections at  $\beta^*$  values close to 1 m. In order to reach a  $\beta^*=1 \text{ m}$  in the ramp and squeeze it is recommended to extend the AC dipole plateau and to provide tools to reconstruct the machine status at any given time.

A  $\beta^*=0.4 \text{ m}$  was already demonstrated in 2012 with two different optics concepts. Achieving  $\beta^*=0.3 \text{ m}$  should be equally feasible. It is recommended to make available all IR non-linear correctors as they can significantly improve the DA at these low  $\beta^*$  values. If the arc MO octupoles were not strong enough to suppress instabilities the IR octupoles could be used to considerably enhance the amplitude detuning. However the DA could also be severely reduced and therefore compromises should be adopted. The two bunch spacing configurations of 25 ns and 50 ns have been considered for luminosity evaluations. The 25 ns bunch spacing tends to give a 20% lower peak luminosity than the equivalent  $\beta^*$  setting at 50 ns.

## 15 ACKNOWLEDGMENTS

We would like to thank the following people for their contributions and discussions: O.E. Berrig, R. Bruce, S. Fartoukh, M. Giovannozzi, B. Goddard, W. Herr, D. Jacquet, V. Kain, A. Macpherson, N. Magnin, R. de Maria, R. Miyamoto, N. Mounet, T. Pieloni, M. Poger, S. Redaelli, F. Schmidt, M. Solfaroli, E. Todesco and J. Wenninger.

## 16 REFERENCES

- [1] Optics Measurements, Corrections and Modeling for High-Performance Storage Rings, June 2011, CERN. <https://indico.cern.ch/conferenceDisplay.py?confId=132526>
- [2] Y.T. Yan, Y. Cai, F-J. Decker, J. Irwin, J. Seeman, S. Ecklund, M. Sullivan, J. Turner, U. Wienands, “PEP-II Beta Beat Fixes with MIA”, SLAC-PUB-10369, 2004.
- [3] P. Castro, “Applications of the 1000-turns Orbit Measurement System at LEP”, Proceedings of the 1999 Particle Accelerator Conference, New York, 1999.
- [4] A. Morita, H. Koiso, Y. Ohnishi and K. Oide, “Measurement and correction of on- and off-momentum beta functions at KEKB”, Phys. Rev. ST Accel. Beams **10**, 072801 (2007).
- [5] D. Sagan, R. Meller, R. Littauer, and D. Rubin, “Betatron phase and coupling measurements at the Cornell Electron/Positron Storage Ring”, Phys. Rev. ST Accel. Beams **3**, 092801 (2000).
- [6] F. Brinker, H. Burkhardt, W. Decking, K. Ehert, W. Fischer, M. Funcke, E. Gianfelice, S. Herb, G.H. Hoffstaetter (editor), U. Hurdelbrink, W. Kriens, C. Montag, F. Schmidt, F. Stulle, R. Tomás, E. Vogel, M. Werner, A. Xiao, “HERA Accelerator studies 2000”, DESY HERA 00-07.
- [7] A. Jansson, P. Lebrun, J.T. Volk, “Beta function measurement in the Tevatron using quadrupole gradient modulation”, Proceedings of PAC 2005, Knoxville, Tennessee.
- [8] G. Vanbavincz, M. Bai, G. Robert-Demolaize, “Optics corrections at RHIC”, Proceedings of IPAC 2011, San Sebastián, Spain.
- [9] I.P.S. Martin, R. Bartolini, R. Fielder, E. Longhi, B. Singh, “Electron beam dynamics studies during commissioning of the DIAMOND storage ring”, Proceedings of PAC07, Albuquerque, New Mexico, USA. “Further advances in understanding and optimising beam dynamics in the DIAMOND storage ring”, Proceedings of EPAC08, Genoa, Italy.
- [10] L.S. Nadolski, “Use of LOCO at synchrotron SOLEIL”, Proceedings of EPAC08, Genoa, Italy.
- [11] G. Benedetti, D. Einfeld, Z. Martí, M. Muñoz, “LOCO in the ALBA storage ring”, Proceedings of IPAC 2011, San Sebastián, Spain.
- [12] R. Tomás, M. Aiba, C. Alabau, O. Brüning, R. Calaga, M. Giovannozzi, V. Kain, P. Hagen, M. Lamont, R. Miyamoto, F. Schmidt, M. Strzelczyk and G. Vanbavincz, “The LHC Optics in Practice”, 2<sup>nd</sup> Evian 2010 Workshop on LHC Beam Operation, Evian, 7-9 Dec. 2010, CERN-ATS-2011-017.
- [13] L. Deniau, N. Aquilina, L. Fiscarelli, M. Giovannozzi, P. Hagen, M. Lamont, G. Montenero, R. Steinhagen, M. Strzelczyk, E. Todesco, R. Tomás, W. Venturini Delsolaro and J. Wenninger, “The magnetic model of the LHC during commissioning to higher beam intensities in 2010-2011”, Proceedings of IPAC 2011, San Sebastián, Spain.
- [14] G. Vanbavincz, M. Aiba, R. Calaga, R. Miyamoto and R. Tomás, “Record low  $\beta$ -beat of 10% in the LHC”, Proceedings of IPAC 2011, San Sebastián, Spain.
- [15] R. Assmann, R. Bruce, M. Giovannozzi, M. Lamont, E. Maclean, R. Miyamoto, G. Mueller, G. Papotti, L. Ponce, S. Redaelli, R. Tomás, G. Vanbavincz, J. Wenninger, “Commissioning of the betatron squeeze to 1 m in IR1 and IR5”, CERN-ATS-Note-2012-005 MD
- [16] E. Meschi, “Luminosity comparison for ATLAS and CMS” 129<sup>th</sup> LHC Machine Committee meeting held on 18 April 2012.
- [17] J. Serrano and M. Cattin, “The LHC AC Dipole system: an introduction”, CERN-BE-Note-2010-014 (CO).
- [18] R. Tomás, T. Bach, R. Calaga, A. Langner, Y.I. Levinsen, E.H. Maclean, R. Miyamoto, T.H.B. Persson, P.K. Skowronski, M. Strzelczyk and G. Vanbavincz, “Record low  $\beta$ -beating in the LHC”, Phys. Rev. ST Accel. Beams **15**, 091001 (2012).
- [19] R. Tomás, “Optimizing the global coupling knobs for the LHC”, CERN-ATS-Note-2012-019 MD.
- [20] A. Boccardi, M. Gasior, O. R. Jones, P. Karlsson, R. J. Steinhagen, “First Results from the LHC BBQ Tune and Chromaticity Systems”, CERN LHC-Performance-Note-007 (2008)
- [21] O. Brüning, P. Collier, P. Lebrun, S. Myers, R. Ostojic, J. Poole and P. Proudlock, “LHC design report”, CERN-2004-003-V-1.
- [22] S. Fartoukh, “Chromatic Coupling Induced by Skew Sextupolar Field Errors in the LHC Main Dipoles and its Correction”, CERN-LHC-Project-Report-278, 1999.
- [23] S. White, E.H. Maclean and R. Tomás, “Direct measurement of amplitude detuning with AC dipoles”, to be published.
- [24] S. Fartoukh, V. Kain, Y. Levinsen, E. Maclean, R. de Maria, T. Person, M. Pojer, L. Ponce, P. Skowronski, M. Solfaroli, R. Tomás and J. Wenninger, “The 10 cm beta\* ATS MD”, CERN-ATS-Note-2013-004 MD.
- [25] L. Jin and F. Schmidt, “Dynamic Aperture tune scan for LHC version 5 at injection energy”, LHC Project Note 182 (1998).
- [26] S. Fartoukh, M. Giovannozzi, “Dynamic aperture computation for the as-built CERN Large Hadron Collider and impact of main dipoles sorting” NIM-A, **671**, 2012.
- [27] R. Calaga, D. Jacquet, E. Metral, R. Miyamoto, N. Mounet, L. Ponce, S. Redaelli, B. Salvant, F. Schmidt, R. Steinhagen, R. Tomás, G. Vanbavincz, and F. Zimmermann, “Collision tunes at injection and ramp”, CERN-ATS-Note-2011-034 MD (LHC).
- [28] M. Giovannozzi, “OPTICS OPTIONS FOR THE 2012 PROTON RUN”, Proceedings of Chamonix 2012 workshop on LHC Performance.
- [29] S. Redaelli, M. Lamont, G. Müller, N. Ryckx, R. Tomás and J. Wenninger, “Combined ramp and squeeze at the Large Hadron Collider”, CERN-ATS-2012-102.